J Mater Sci: Mater Electron (2017) 28:7686–7691
DOI 10.1007/s10854-017-6462-0

In situ synthesis of silver/chemically reduced graphene nanocomposite and its use for low temperature conductive paste

Bin Feng[1,2] · Xiaolong Gu[1] · Xinbing Zhao[2] · Yu Zhang[1] · Tianyu Zhang[1] · Jinguang Shi[1]

Received: 21 November 2016 / Accepted: 25 January 2017 / Published online: 6 February 2017

Abstract In this work, we succeeded in the synthesis of Ag/chemically reduced graphene (Ag/G) nanocomposite by a facile in situ one-pot solvothermal route. X-ray diffraction, X-ray photoelectron spectroscopy, Raman spectra and Fourier transform infrared spectroscopy results revealed the formation of Ag and the reduction of graphite oxide to graphene during the one-pot process. Scanning electron microscopy observation indicated that spherical Ag particles with a size less than 100 nm are wrapped by graphene. The Ag/G nanocomposite was used in a low temperature conductive paste. Thermal analysis was conducted to determine the proper curing process of the Ag/G conductive paste. The Ag/G conductive paste that contains 0.6 wt% graphene exhibits low sheet resistance (22 mΩ/sq/25 μm) and good stability after cured at 150 °C for 30 min, which made us believe that the Ag/G nanocomposite is a promising candidate for conductive paste.

1 Introduction

Conductive paste, which is used to fabricating conductive patterns on different substrates by screen printing, has important applications in many fields, such as touch panels [1], solar cells [2], flexible printing electric devices [3], organic light emitting device [4] (OLED) and so on. Hence, how to synthesize conductive phase and prepare conductive pastes has received much attention in current researches. In most pastes, the precious metal silver is traditionally used as a high performance conductive phase because of its high electrical conductivity and stability. However, due to the high cost and scarcity of silver, there is a need to develop suitable replacements for pure silver. In addition, the performances of conductive paste with new conductive phase should be comparable with those Ag conductive pastes.

To date, one of the strategies is to replace the Ag with less-expensive metals, such as Cu [5] and Ni [6]. Conductive pastes contain less-expensive metals exhibit good electrical conductivities while lack of stability. Carbon materials is another choice to replace Ag. However, carbon based conductive pastes [7, 8] are disadvantage in electrical conductivity even though they show good stability. Except for these two methods, using composites made of Ag and carbon materials as conductive phase seems to be a better route, which have been proved by some research work [9–12].

Compared with conventional carbon materials, graphene, a sp^2-bonded two-dimensional (2D) carbon material, is more attractive as a component of composite due to its high electronic conductivity [13], high specific surface area [14] and high mechanical strength [15]. Herein, we report a facile preparation of Ag/chemically reduced graphene (Ag/G) nanocomposite by an in situ one-pot solvothermal route and demonstrate its use in conductive paste. Via in-situ solvothermal process, spherical Ag particles with a size less than 100 nm are wrapped by graphene. It was found that conductive paste contain this nanocomposite exhibits low sheet resistance and good stability after cured, which made us believe that the Ag/G nanocomposite is competent for preparation of conductive paste.

✉ Bin Feng
Binfeng@asia-general.com

[1] Zhejiang Province Key Laboratory of Soldering & Brazing Materials and Technology, Zhejiang Metallurgical Research Institute Co., Ltd., Hangzhou 310030, China

[2] State Key Laboratory of Silicon Materials and Department of Materials Science and Engineering, Zhejiang University, Hangzhou 310027, China

2 Experiments

2.1 Synthesis of Ag/G nanocomposite

For the preparation of the Ag/G nanocomposites, graphite oxide (GO) (25 and 50 mg for different samples), synthesized by the modified Hummer's method, was ultrasonically dispersed in 50 mL of deionized water for 2 h to get exfoliated graphene oxide using an ultrasonic bath. Subsequently, 1.25 mmol of $AgNO_3$ was added to the above solution. After being stirred for 2 h, moderate $NH_3{\cdot}H_2O$ was added to the above solution to adjust the PH value of nine. And the desire amount of $N_2H_4{\cdot}H_2O$ was added slowly to the above mixed solution which was then further stirred for 0.5 h. The resultant product was separated by centrifugation, washed with deionized water and dried at 40 °C under vacuum overnight. For comparison, bare Ag was prepared using the similar route without adding GO. Chemically reduced graphene was also prepared by a similar procedure.

2.2 Preparation of conductive paste

The conductive paste contained 60 wt% Ag/G nanocomposite, 11 wt% resin (polyester resin) and 29 wt% organic solvent (mixture of propylene glycol phenyl ether and carbitol acetate). Typically, the resin and the organic solvent were mixed in a three-necked round-bottom flask for 10 h at 90 °C, cooled to the room temperature. And then the Ag/G nanocomposite was added to the mixture of the resin and solvent and mixed for 5 min by a planetary centrifugal mixer to be a conductive paste. The paste was then passed through a zirconia triple roller mill to break the agglomerates. This process was repeated several times to obtain a homogeneous paste with a degree of fineness under 10 μm. Different pastes were prepared with different graphene content. The corresponding weight percentage of graphene are 0.3% and 0.6% respectively. For comparison, paste with pure Ag was also prepared using the similar route. By using a screen printing method, the pastes were applied to a paper substrate. And the curing process was conducted under 150 °C for 30 min. The printed tracks were heated in an electric oven at 80 °C for 10 days for measurement of sheet resistance.

2.3 Materials characterizations

The crystalline structures of the products were characterized by X-ray diffraction (XRD) on a Bruker D8 Advance powder diffractometer equipped with Cu Kα radiation (λ = 1.54 Å). The morphologies of the products were observed by field emission scanning electron microscopy (SEM) on a EIGMA microscope, X-ray photoelectron spectroscopy (XPS) measurements were performed on a KRATOS AXIS ULTRA-DLD spectrometer with a monochromatic Al Kα radiation (hυ = 1486.6 eV). Raman spectra were recorded on a Jobin-Yvon Labor Raman HR-800 Raman system by exciting a 514.5 nm Ar^+ laser. Fourier transform infrared spectroscopy (FTIR) measurements were performed on a Nicolet 6700 Fourier infrared spectrometer. The powder sample was mixed uniformly with KBr at a weight ratio of 1:100, and pressed into a pellet before FTIR measurements. The carbon content analysis was conducted on a CS-2800 carbon sulphur analyzer. The viscosity of the Ag/G pastes were measured by Malcom PCU205 Viscometer at 10 rpm at 25 °C. And the viscosity of the Ag/G pastes were in the range of 200–400 Pa/s. Measurement of sheet resistance were performed with a RTS-8 four-probe meter at 25 °C. And the thickness of the trace were measured by SEM.

3 Results and discussion

Figure 1a shows the XRD patterns of the Ag/G nanocomposite and bare Ag. The dominant diffraction peaks can be indexed to Ag (space group *Fm*3m, JCPDS No. 04-0783) for both Ag/G nanocomposite and bare Ag. The diffraction peak of GO was not observed in Ag/G which indicated that GO was reduced into graphene during the reduction process [16]. And the concentration of graphene is estimated to be 1 wt% by carbon content analysis.

Figure 1b gives the Raman spectra of Ag/G, graphene and GO. For all the three samples, two bands at 1350 and 1580 cm^{-1} appear, corresponding to the disordered (*D*) and graphitic (*G*) bands of carbon-based materials [17]. The *D*-to-*G* peak intensity ratios of GO, bare graphene and graphene in Ag/G are calculated to be 0.79, 1.11 and 1.06, respectively. Note that, compared with GO, both Ag/G and graphene exhibit an increased *D*/*G* intensity ratio, which is caused by a reduction of the average size of the sp^2 domains and an increased number of these domains, indicating the reduction of GO to graphene [18]. It should be noted that the *G* peak shows an asymmetric feature. In fact, it consists of two overlapped peaks, namely, *G* and *D′* bands, located at 1580 and 1620 cm^{-1}, respectively. The *D′* peak is a defect peak due to intra-valley scattering [17]. The asymmetric feature of *G* peak of graphene was also observed in other work [19, 20]. The peaks at around 2700 and 2900 cm^{-1} are related to 2*D* mode [21] and *D* + *G* mode [22], respectively, of carbon-based materials. Note that Ag/G exhibits a broad 2*D* peak, indicating the few-layer feature of graphene [21]. Broad 2*D* peak was also observed in few-layer graphene prepared by either solution chemical route [23] or chemical vapor deposition (CVD) [24]. Raman spectra only give the statistical average of the powder sample, where a large number of graphene sheets

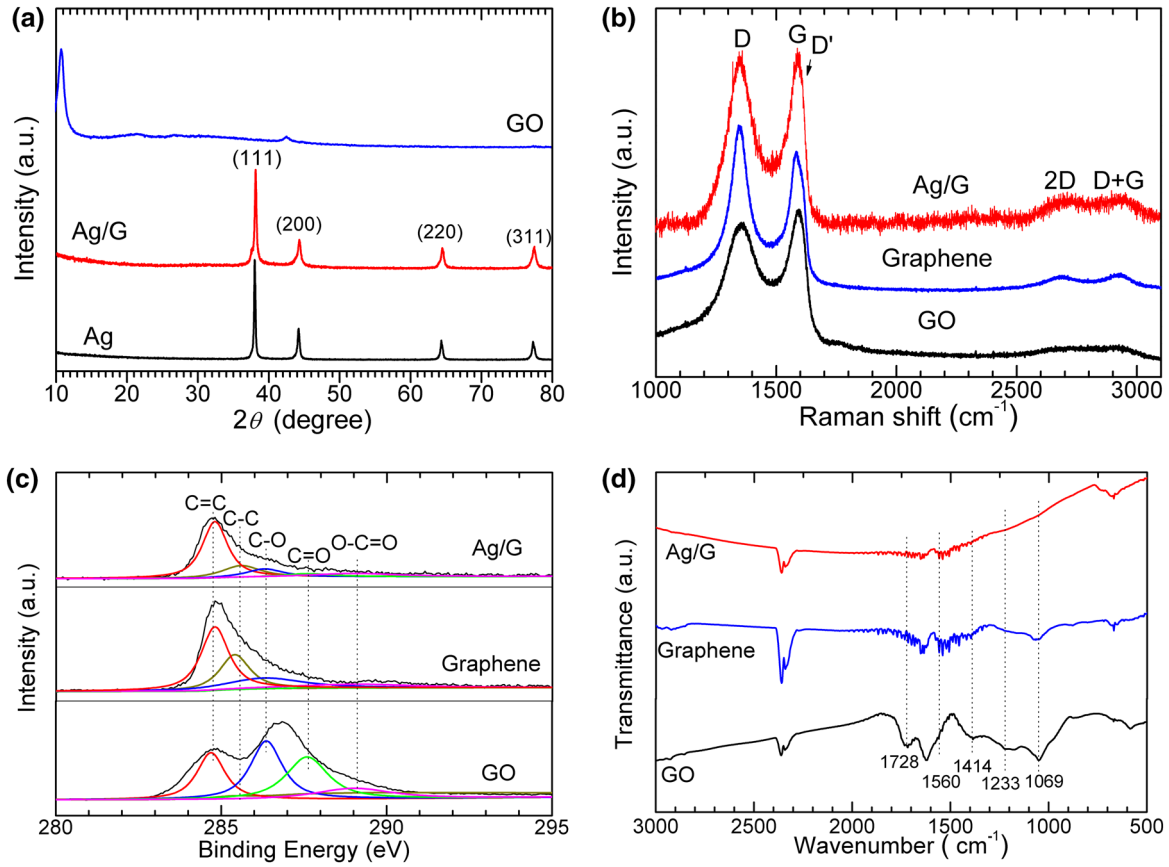

Fig. 1 **a** XRD patterns of GO, Ag/G and bare Ag, **b** Raman spectra of Ag/G, graphene and GO, **c** C1s XPS of Ag/G, graphene and GO and **d** FTIR of Ag/G, graphene and GO

in single-, double- or few-layer form coexist in the powder. It should be stressed that when defined in a general sense, "graphene" can be distinguished as three different types: single-, double-, and few layer (3 to <10 layers) according to Geim et al. [25]. In this sense, the graphene in Ag/G can be regarded as "graphene" in few-layer form.

Figure 1c presents the C1s XPS of Ag/G,graphene and GO. The XPS is fitted into five peaks, corresponding to carbon atoms in four functional groups: non-oxygenated carbon (C–C 285.6 eV or C=C 284.8 eV), carbon in C–O group (epoxide or hydroxyl, 286.3 eV), carbonyl carbon (C=O 287.6 eV) and carboxylate carbon (O–C=O, 289.0 eV) [18, 26]. Note that the peak intensity of carbons in C–O, C=O and O–C=O groups exhibits a significant decrease in Ag/G and graphene compared with that in GO, indicative of a sufficient reduction of GO into graphene. Note that the solvothermal products still contain residual epoxide and/or hydroxyl groups, in consistent with the theoretical calculation that these groups are difficult to be removed when located at the edges of the GO [27].

The samples were further checked by FTIR to check the reduction status of GO as indicated in Fig. 1d. For GO, the strong absorption band at 1724 cm^{-1} is due to the C=O stretching, the band around 1622 cm^{-1} due to aromatic C=C, while the bands at 1412, 1233, and 1060 cm^{-1} correspond to carboxy C–O, epoxy C–O and alkoxy C–O, respectively [28]. Of note is the obvious decrease of the peak intensity related to C=O and C–O, indicative of remarkable reduction of GO after the solvothermal reactions, agreeing well with the Raman and XPS results.

The microstructure of Ag/G nanocomposite and bare Ag was characterized by SEM as shown in Fig. 2. Figure 2a show typical SEM of Ag/G nanocomposite, indicating nano-sized Ag particles are warpped by graphene sheet. The graphene sheet exhibits a transparent feature as denoted by the arrows, indicating that it is rather thin. The microstructure of bare Ag was also characterized to check the effect of graphene on the morphology. Note that bare Ag crystals tend to aggregate without the dispersing and confining effects of graphene as shown in Fig. 2b.

The schematic of the preparation and curing process of the Ag/G conductive paste is shown in Fig. 3a. The Ag/G nanocomposite was blended with organic mixture to form the conductive paste. After dispersed by a three-roller mill,

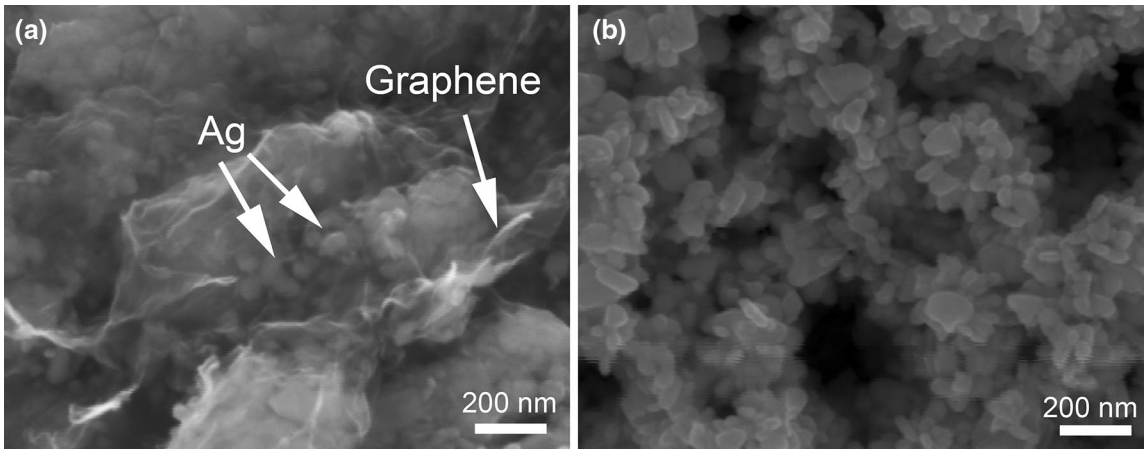

Fig. 2 SEM images of **a** Ag/G nanocomposite and **b** bare Ag

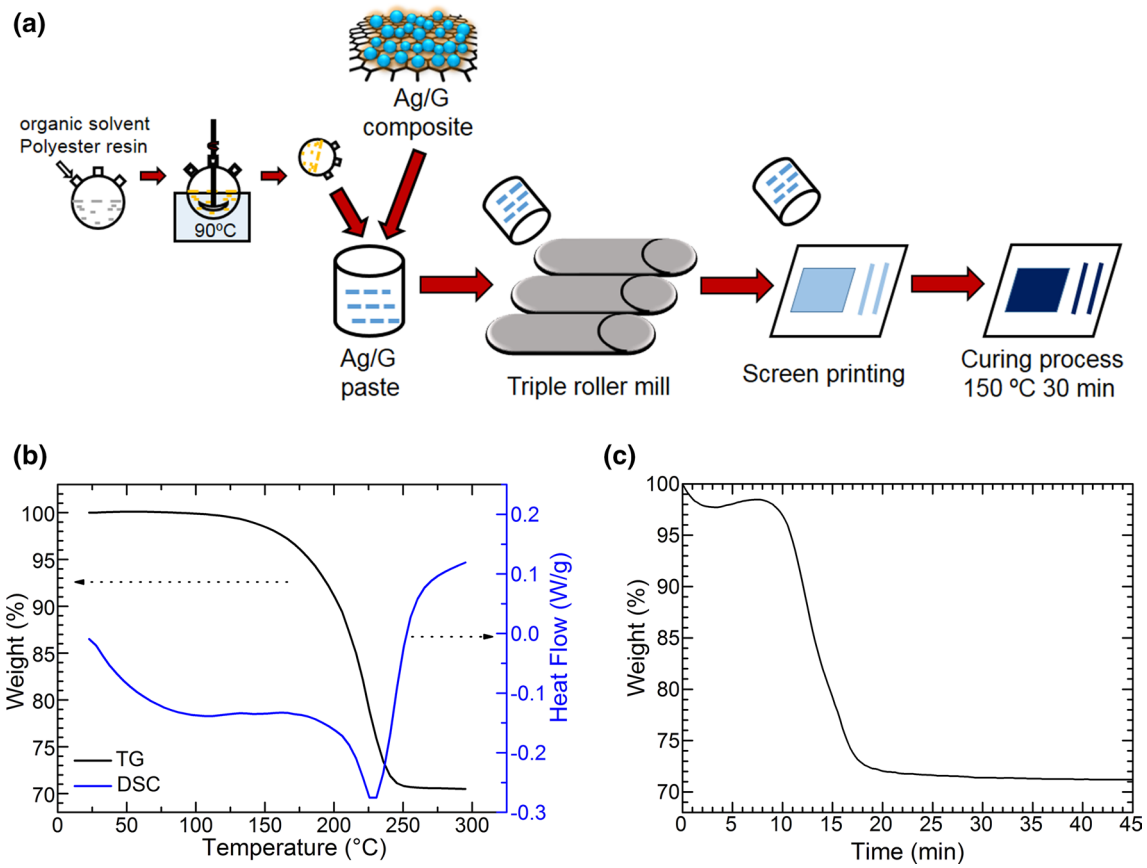

Fig. 3 **a** Schematic illustration of the the preparation and curing process of the Ag/G conductive paste and **b** TGA curves of the Ag/G conductive paste, and **c** TGA isotherms at specified temperatures of 150 °C

the paste can be easily printed on substrates for further curing process. Thermal analysis was conducted to determine the proper curing process. Figure 3b gives the TGA and DSC curves of the Ag/G conductive paste. An obvious mass loss observed between 150 and 245 °C corresponded to evaporation of the solvents. And an apparent exothermic peak appeared at the heating temperature about 225 °C, which indicated the state of the conductive paste changed and the curing process was completed at 225 °C. Isothermal TGA measurement at 150 °C indicate that all the solvent

will evaporate (asymptotic at 71%) after about 18 min. Therefore, the conductive paste was cured at 150 °C for 30 min to ensure the solvent volatilize completely and the resin cure fully.

The conductivity of the synthesized Ag/G nanocomposites is the most important thing we care about, which decides whether the Ag/G nanocomposite is suitable for conductive paste or not. Figure 4 exhibit the photos of printed tracks on paper substrate. The printed tracks were used as a part of an electrical circuit as shown in Fig. 4a. When the traces were electrified from the end point, the LED was lighted, indicating a good electrical conductivity of the traces, as demonstrated in Fig. 4b. In addition, the Ag/G conductive paste is also fit for printing fine line pattern and irregular pattern. Figure 4c shows the good electrical conductivity of the trace of a line pattern with width of 300 μm and Fig. 4d shows the case for an irregular pattern. The sheet resistance of Ag/G conductive pastes that contain 0.3 and 0.6 wt% graphene are 32 mΩ/sq/25 μm and 22 mΩ/sq/25 μm. And the sheet resistance of conductive paste without graphene is 37 mΩ/sq/25 μm. Note that the Ag/G pastes show a better electrical property than pure Ag paste prepared by the same method. The sheet resistance of Ag/G conductive pastes is even comparable with some commercial products, such as Heraeus Ag paste LTC 3601 (15 mΩ/sq/25 μm) and Engineered Conductive Materials CI-1035c (35 mΩ/sq/25 μm). In addition, the Ag/G paste also exhibit good thermal stability and oxidation resistance. The printed tracks were heated in an electric oven at 80 °C for 10 days and the sheet resistance remain the same.

Figure 5 show cross-section SEM images of the printed track of the Ag/G paste. As shown in Fig. 5a, most of the Ag particles had fused together and connected with graphene to form a network throughout the entire film. Figure 5b gives a magnified image. The silver particles can be clearly identified. Between neighboring Ag particles or clusters, there were gaps. These gaps were much smaller than the size of graphene and thus the Ag particles were easily connected by the graphene sheets.

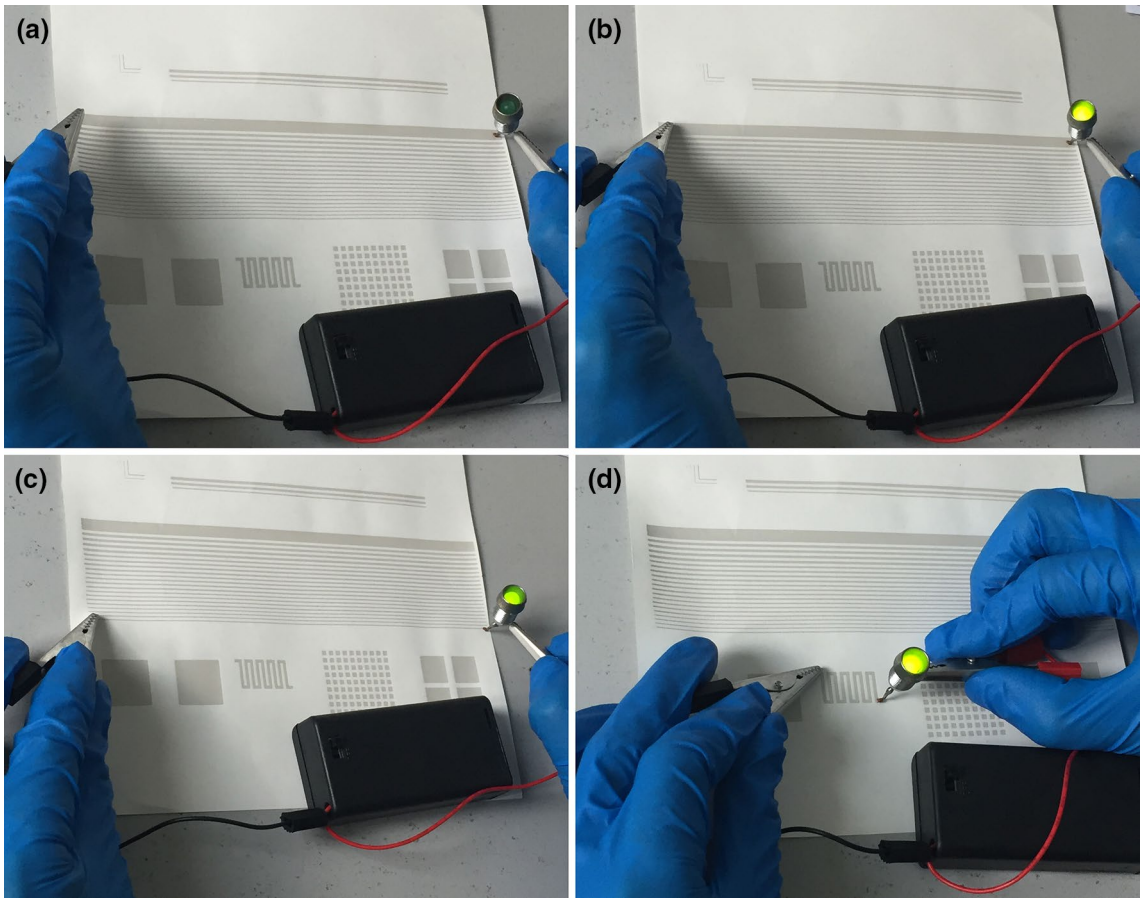

Fig. 4 Photos of printed tracks on paper substrate: **a** the trace was not electrified from the end point, **b** a line pattern with width of 4 mm, **c** a line pattern with width of 300 μm and **d** an irregular pattern were electrified from the end point, LED was lighted

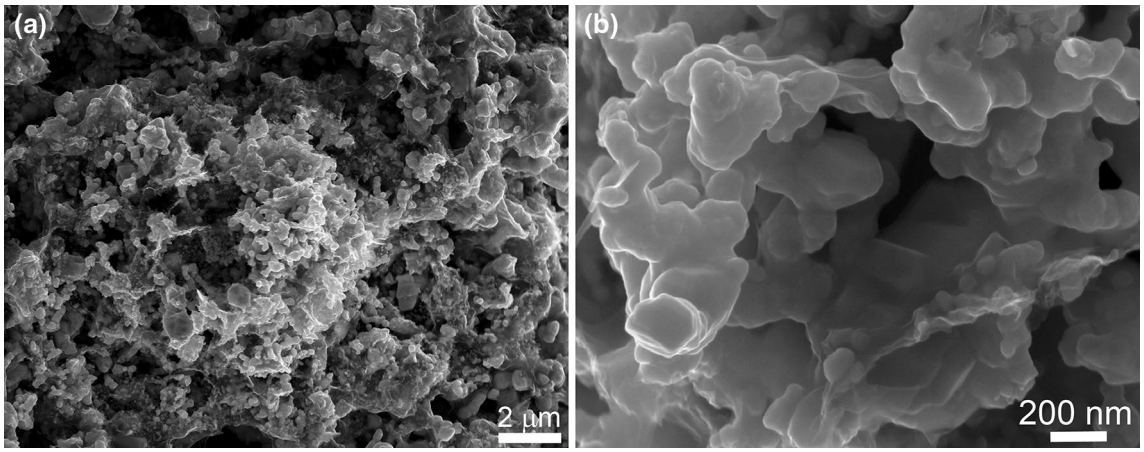

Fig. 5 **a** Cross-section SEM images of the printed track of the Ag/G paste and **b** magnified image of the printed track of the Ag/G paste

4 Conclusion

In summary, Ag/G nanocomposite has been synthesized by a simple in situ one-pot solvothermal route. Spherical Ag particles with a size less than 100 nm are wrapped by graphene. The Ag/G nanocomposite was used in a low temperature conductive paste. Thermal analysis was conducted to determine the proper curing process of the Ag/G conductive paste. The paste exhibits low sheet resistance (22 mΩ/sq/25 μm) after cured at 150 °C for 30 min, which made us believe that the Ag/G nanocomposite is a promising candidate for conductive paste.

Acknowledgements This work was supported by the Science and Technology Project of Zhejiang Province (Nos. 2016F50055, 2016F50057).

References

1. J. Kwon, H. Cho, H. Eom, H. Lee, Y.D. Suh, H. Moon, J. Shin, S. Hong, S.H. Ko, Acs Appl. Mater. Inter. **8**(18), 11575 (2016)
2. S.H. Ko, Smart Sci. **2**(2), 54 (2014)
3. J. Liu, C. Yang, P. Zou, R. Yang, C. Xu, B. Xie, Z. Lin, F. Kang, C.P. Wong, J. Mater. Chem. C **3**(32), 8329 (2015)
4. S.J. Kim, K. Choi, S.Y. Choi, J. Korean. Phys. Soc. **68**(6), 779 (2016)
5. S.K. Tam, K.M. Ng, J. Nanopart. Res. **17**(12), 12 (2015)
6. H.R. Qin, J.M. Xie, J.J. Jing, W.H. Li, Z.F. Jiang, in *Renewable and Sustainable Energy, Pts 1–7*, ed. by W. Pan, J.X. Ren, Y.G. Li (Trans Tech Publications Ltd, Dürnten, 2012), pp. 3485
7. K. Hu, S.Z. Liu, J.X. Lei, C.L. Zhou, Polym. Compos. **36**(3), 467 (2015)
8. V.H.R. Souza, S. Husmann, E.G.C. Neiva, F.S. Lisboa, L.C. Lopes, R.V. Salvatierra, A.J.G. Zarbin, Electrochim. Acta **197**, 200 (2016)
9. W. Wu, S.L. Yang, S.F. Zhang, H.B. Zhang, C.Z. Jiang, J. Colloid Interface Sci. **427**, 15 (2014)
10. Y.G. Hu, T. Zhao, P.L. Zhu, Y. Zhu, X.T. Shuai, X.W. Liang, R. Sun, D.D. Lu, C.P. Wong, J. Mater. Chem. C **4**(24), 5839 (2016)
11. P.A. Hu, W. O'Neil, Q. Hu, Appl. Surf. Sci. **257**(3), 680 (2010)
12. V. Brusic, G.S. Frankel, J. Roldan, R. Saraf, J. Electrochem. Soc. **142**(8), 2591 (1995)
13. S. Iijima, T. Ichihashi, Nature **363**(6430), 603 (1993)
14. H.K. Kim, F.G. Shi, Microelectronic. J. **32**(4), 315 (2001)
15. A.I. Medalia, Chem. Technol. **59**(3), 432 (1986)
16. L.F. Zhang, C.Y. Zhang, Nanoscale **6**(3), 1782 (2014)
17. A.C. Ferrari, Solid State Commun. **143**(1–2), 47 (2007)
18. S. Stankovich, D.A. Dikin, R.D. Piner, K.A. Kohlhaas, A. Kleinhammes, Y. Jia, Y. Wu, S.T. Nguyen, R.S. Ruoff, Carbon **45**(7), 1558 (2007)
19. D. Chen, W. Wei, R. Wang, J. Zhu, L. Guo, New J. Chem. **36**(8), 1589 (2012)
20. G. Wang, B. Wang, X. Wang, J. Park, S. Dou, H. Ahn, K. Kim, J. Mater. Chem. **19**(44), 8378 (2009)
21. A.C. Ferrari, J.C. Meyer, V. Scardaci, C. Casiraghi, M. Lazzeri, F. Mauri, S. Piscanec, D. Jiang, K.S. Novoselov, S. Roth, A.K. Geim, Phys. Rev. Lett. **97**(18), 187401 (2006)
22. C.N.R. Rao, A.K. Sood, K.S. Subrahmanyam, A. Govindaraj, Angew. Chem. Int. Ed. **48**(42), 7752 (2009)
23. G. Wang, J. Yang, J. Park, X. Gou, B. Wang, H. Liu, J. Yao, J. Phys. Chem. C **112**(22), 8192 (2008)
24. K.S. Kim, Y. Zhao, H. Jang, S.Y. Lee, J.M. Kim, K.S. Kim, J.H. Ahn, P. Kim, J.Y. Choi, B.H. Hong, Nature **457**(7230), 706 (2009)
25. F. Schedin, A.K. Geim, S.V. Morozov, E.W. Hill, P. Blake, M.I. Katsnelson, K.S. Novoselov, Nat. Mater. **6**(9), 652 (2007)
26. H.J. Shin, K.K. Kim, A. Benayad, S.M. Yoon, H.K. Park, I.S. Jung, M.H. Jin, H.K. Jeong, J.M. Kim, J.Y. Choi, Y.H. Lee, Adv. Funct. Mater. **19**(12), 1987 (2009)
27. X. Gao, J. Jang, S. Nagase, J. Phys. Chem. C **114**(2), 832 (2009)
28. S. Park, J. An, I. Jung, R.D. Piner, S.J. An, X. Li, A. Velamakanni, R.S. Ruoff, Nano Lett. **9**(4), 1593 (2009)